

SAND77-1789  
Unlimited Release

**MASTER**

## Duopigatron Ion Source Studies

Frank M. Bacon, Robert W. Bickes, Jr., James B. O'Hagan



Sandia Laboratories

## ACKNOWLEDGMENTS

Many of the duopigatron ion source parts were obtained from O. B. Morgan and R. C. Davis at ORNL. Helpful discussions with G. W. McClure are gratefully acknowledged.

NOTICE

This report was prepared as an account of work sponsored by the United States Government. Neither the United States nor the United States Department of Energy, nor any of their employees, nor any of their contractors, subcontractors, or their employees, make any warranty, express or implied, or assumes any legal liability or responsibility for the accuracy, completeness or usefulness of any information, apparatus, product, process disclosed, or represents that its use would not infringe privately owned rights.

NOTICE **IN ONLY**

**PORTIONS OF THIS REPORT ARE ILLEGIBLE. It has been reproduced from the best available copy to permit the broadest possible availability.**

26

**DISTRIBUTION OF THIS DOCUMENT IS UNLIMITED**

SAND77-1789  
UNLIMITED RELEASE  
Printed July 1978

DUOPIGATRON ION SOURCE STUDIES\*

Frank M. Bacon  
Tube Development Division 2351

Robert W. Bickes, Jr.  
James B. O'Hagan  
Atomic and Arc Physics Division 2352

Sandia Laboratories  
Albuquerque, New Mexico 87115

ABSTRACT

Ion source performance characteristics consisting of total ion current, ion energy distribution, mass distribution, and ion current density distribution have been measured for several models of a duopigatron. Variations on the duopigatron design involved plasma expansion cup material and dimensions, secondary cathode material, and interelectrode spacings. Of the designs tested, the one with a copper and molybdenum secondary cathode and a mild steel plasma expansion cup proved to give the best results. The ion current density distribution was peaked at the center of the plasma expansion cup and fell off to 80% of the peak value at the cup wall for a cup 15.2 mm deep. A total ion current of 180 mA consisting of 60-70% atomic ions was produced with an arc current of 20 A and source pressure of 9.3 Pa. More shallow cups produced a larger beam current and a more sharply peaked ion current density distribution. Typical ion energy distributions were bell-shaped curves with a peak 10 to 20 V below anode potential and with ion energies extending 30 to 40 V on either side of the peak.

---

\*Work Sponsored by U. S. Department of Energy.

## TABLE OF CONTENTS

	<u>Page</u>
I. INTRODUCTION . . . . .	5
II. EXPERIMENTAL APPARATUS . . . . .	5
III. EXPERIMENTAL RESULTS . . . . .	8
A. <u>Model 1.</u> . . . . .	8
Table I. . . . .	10
B. <u>Model 2.</u> . . . . .	11
C. <u>Model 3.</u> . . . . .	11
D. <u>Model 4.</u> . . . . .	14
E. <u>Model 5.</u> . . . . .	14
F. <u>Models 6 and 7.</u> . . . . .	17
G. <u>Models 8, 9, and 10.</u> . . . . .	17
IV. DISCUSSIONS AND CONCLUSIONS . . . . .	23
LIST OF REFERENCES . . . . .	25

LIST OF FIGURES

<u>Figure No.</u>	<u>Page</u>
1. Schematic Drawing of Duopigatron Ion Source. . .	6
2. Experimental Data Obtained on Duopigatron - Model 1. . . . .	9
3. Experimental Data Obtained on Duopigatron - Model 2. . . . .	12
4. Experimental Data Obtained for Duopigatron - Model 3. . . . .	13
5. Experimental Data Obtained for Duopigatron - Model 4. . . . .	15
6. Experimental Data Obtained on Duopigatron - Model 5. . . . .	16
7. Experimental Data Obtained on Duopigatron - Model 6. . . . .	18
8. Experimental Data Obtained for Duopigatron - Model 7. . . . .	19
9. Experimental Data Obtained for Duopigatron - Model 8. . . . .	20
10. Experimental Data Obtained for Duopigatron - Model 9. . . . .	21
11. Experimental Data Obtained for Duopigatron - Model 10 . . . . .	22



## I. INTRODUCTION

As recently reported,<sup>1</sup> the ion production characteristics of a duoplasmatron ion source were shown to be improved if a Penning type discharge was induced in the plasma expansion cup by allowing the cup to float electrically and if the anode hole was enlarged from its original diameter. These results indicated that a duopigatron ion source may be an improvement over the duoplasmatron. Original work on the duopigatron ion source was reported by Demirkhanov, et al.,<sup>2</sup> and Morgan, et al.,<sup>3</sup> The Demirkhanov group obtained ion beam currents of over 1 A that were 85% H<sup>+</sup> ions in a pulsed discharge. Morgan, et al., modified the design for continuous operation and to increase the molecular ion content in the beam.

The main ion source requirements for the Sandia neutron source target test facility, briefly described in Ref. 1, are a continuously operating, 200 mA ion beam optimized for atomic deuterium ion production and for uniformity in the ion current density distribution in the plane of the exit aperture of the ion source. Ten variations on the duopigatron ion source design are described in this report. The effects of design changes on the total ion beam current, the ion mass and energy distributions, and ion current density distributions are reported. The purpose of the experiments detailed here was not a precise evaluation of the physics of the duopigatron ion source, but rather to carry out systematic investigations of easily changed source parameters (arc current, gas pressure, and electrode geometry) in order to obtain a deuterium ion beam with the required characteristics.

## II. EXPERIMENTAL APPARATUS

The first ion source configuration investigated, shown in Fig. 1, was based on the Demirkhanov, et al.,<sup>2</sup> design. The cathode, electromagnet, and intermediate electrode were the same used in recent duoplasmatron studies<sup>1</sup>; however, the exit aperture of the intermediate electrode was enlarged to

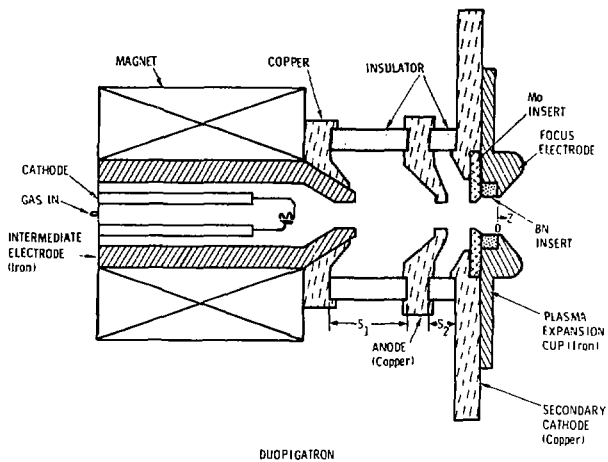


Figure 1. Schematic Drawing of Duopigatron Ion Source.

8.8 mm diameter for the duopigatron. The copper anode for the duopigatron had a 7.1 mm diameter aperture and was separated on axis 29.2 mm from the intermediate-electrode with an alumina spacer,  $S_1$ , 30.5 mm long. The axial distance between the anode and secondary cathode was 2.2 mm less than the alumina spacer length  $S_2$  which was 12.7 mm for the design shown in Fig. 1. A molybdenum insert was used in the center of the copper secondary cathode to minimize erosion of this electrode by the arc discharge. Plasma flowed from the arc discharge through a 6.7 mm diameter aperture in the molybdenum insert into the plasma expansion cup, 15.2 mm deep by 12.7 mm inside diameter. The plasma expansion cup shown in Fig. 1 was made of iron and contained a 25.4 mm o.d. boron nitride insert which withstood plasma heating of the cup wall better than iron. For all of the experiments described in this paper, the plasma expansion cup was connected electrically to the secondary cathode. Unless otherwise stated, the secondary cathode was maintained at cathode potential. The design shown in Fig. 1 has a focus electrode, similar to a Pierce electrode, on the plasma expansion cup. This feature was not needed in these experiments, since the ion source was not operated on an ion accelerator, and was not present on all plasma expansion cups tested. The intermediate electrode was connected to the anode with a 100  $\Omega$  resistor and operated near plasma floating potential during the arc discharge. All electrodes and the electromagnet were water cooled. For a magnet current of 2 A, the axial magnetic field near the exit aperture of the intermediate electrode was 0.15 T and near the exit aperture of the plasma expansion cup was 4 mT. Unless otherwise stated, the magnet current for all tests was 2 A. Geometrical variations on the plasma expansion cup and on electrode spacings were made in attempts to achieve a uniform ion current density distribution in the plasma expansion cup, to maximize the atomic ion percentage in the ion beam and to obtain a 200 mA ion beam. Ion source pressure, measured in the cathode region of the ion source with arc off by a capacitance manometer, was 6 to 10 Pa.

Apparatus to measure the ion current density distribution, mass distribution and total beam current was previously described.<sup>1</sup> Corrections to the mass distribution data due to attenuation by background gas were comparable to those for the duoplasmatron.

### [[I. EXPERIMENTAL RESULTS

A summary of the experimental results on each model tested will be presented. An abbreviated version of this report has been published.<sup>4</sup>

#### A. Model 1.

The first model tested was that shown in Fig. 1. Results for the different experiments are shown in Fig. 2. Total ion current was as large as 300 mA at an arc current of 19 A while the atomic ion percentage was about 55%. At a source pressure of 6.7 Pa and over the current range of 12 to 19 A, the atomic ion percentage varied from 50 to 55% while  $D_3^+$  composed 10 to 20% of the sample. At lower arc currents, the  $D_3^+$  was the dominant constituent, composing 95% and 40% of the sample at 4 A and 8 A arc current, respectively; the remainder of the beam sample was evenly divided between  $O^+$  and  $D_2^+$ . The ion current density distribution (shown in Fig. 2 for  $Z = 0$ ) was peaked at the center of the cup with the value at the cup wall about 35% of the peak. Other current density profiles at different values of  $Z$  were measured for use in ion optics calculations.<sup>5</sup> The relative shapes of the distributions were independent of arc current and source pressure over the range investigated. The ion energy distributions relative to cathode potential were bell-shaped curves with a peak about 10 V below anode potential with ion energies extending 30 - 40 V on either side of the peak. All of the energy distributions for the remaining source geometries were essentially the same as described above and will not be further discussed. A summary of the pertinent geometrical parameters for Model No. 1 and the results at 20 A arc current (extrapolated from the data in Fig. 2) and 6.7 Pa source pressure are shown in the first row of Table 1. This table will be used to compare the different models that were tested.

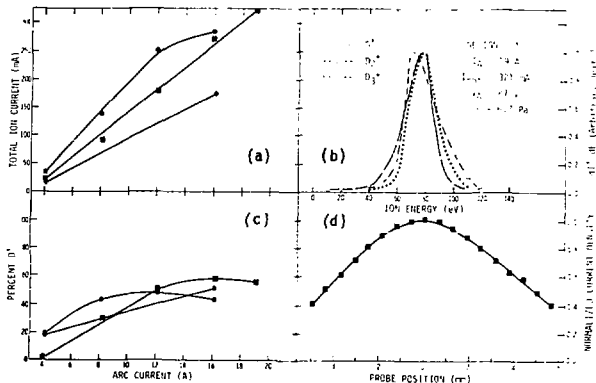


Figure 2. Experimental Data Obtained on Duopigatron - Model 1.

- (a) Total ion current vs. arc current for three source pressures; ● 5.3 Pa; ■ 6.7 Pa; ◆ 8.0 Pa.
- (b) Ion energy distributions for 19 A arc current and 6.7 Pa source pressure. Energy measured relative to cathode potential.
- (c) Percent  $D^+$  vs. arc current for three different source pressures; ● 5.3 Pa; ■ 6.7 Pa; ◆ 8.0 Pa.
- (d) Ion current density distribution in  $Z = 0$  plane of plasma expansion cup for 16 A arc current and source pressure of 6.7 Pa.

Table I. Summary of results from various source geometries. Spacings  $S_1$  and  $S_2$  are defined in Fig. 1. R is ratio of ion current density at edge of plasma cup to current density at center of cup in  $Z = 0$  plane. Intermediate electrode aperture diameter,  $d_{IE}$ , of 6.1 mm.

Model No.	$S_1$ (mm)	$S_2$ (mm)	Secondary Cathode	Cup Material	Cup Depth (mm)	$I^+$ (mA) (a)	% $D^+$ (a, e)	R
1	30.5 <sup>(b)</sup>	12.7	Cu/Mo	Steel/BN	15.2	330 <sup>(d)</sup>	53 <sup>(0)</sup>	0.35
2	30.5	12.7	Cu/Mo	Steel/BN	15.2	350	46	0.35
3	30.5	12.7	Steel	Steel/BN	15.2	200	60	0.55
4	12.7	30.5	Steel	Steel/BN	15.2	185	60	0.5
5	30.5	12.7	Cu/Mo	Steel	15.2	180	66	0.8
6	30.5	38.1	Cu/Mo	Steel	15.2	130	73	0.8
7	38.1	30.5	Cu/Mo	Steel	15.2	120	69	0.75
8	12.7	30.5	Cu/Mo	Steel	15.2	155	60	0.75 <sup>(c)</sup>
9	12.7	30.5	Cu/Mo	Steel	7.6	320	60	0.33
10	12.7	30.5	Cu/Mo	Steel	11.4	215	60	0.50

(a) Source Pressure of 9.3 Pa and arc current of 20 A.

(b)  $d_{IE} = 8.8$  mm

(c) Estimated from Models 5, 6, and 7.

(d) Source pressure of 6.7 Pa.

(e)  $D_3^+$  was 5 to 10% of the sample and  $D_2^+$  composed the remainder of the sample.

### B. Model 2.

The geometry of Model 2 was identical to Model 1 except the intermediate electrode aperture was reduced to 6.1 mm. As a result, the source pressure had to be increased to make the source operate stably at the higher arc currents. Over the pressure range of 6.7 to 9.3 Pa, the total ion current was insensitive to pressure and approximately a linear function of arc current as shown in Fig. 3. At 20 A arc current, the total ion current was about 350 mA. At a source pressure of 9.3 Pa and arc current range of 12 to 20 A, the atomic ion percentage was about 45% and the  $D_2^+$  percentage was 40 to 45%. The ion current density distribution was flatter in the center of the cup than was observed for Model No. 1; however, the relative distribution at the cup walls was the same, as indicated in Table 1. All remaining tests were performed with the 6.1 mm diameter intermediate electrode aperture.

### C. Model 3.

A mild steel secondary cathode was employed on this model to determine how its modification of the magnetic field would affect the ion production characteristics. The Demirkhanov source<sup>2</sup> had used a steel cathode and produced a beam containing 85% atomic hydrogen ions. For a 2 A magnet current, the axial magnetic field at the snout of the intermediate electrode was 0.17 T and was about 2 mT at the exit aperture of the plasma expansion cup. The effects of the mild steel secondary cathode on the ion production characteristics, when compared with Model 2, were to increase the atomic ion percentage, flatten the current density distribution and decrease the total ion current as shown in Table 1 and Fig. 4. At a source pressure of 9.3 Pa and over the arc current range of 12 to 25 A, the atomic ion fraction was 60% and the total ion current ranged from 125 to 240 mA and was approximately a linear function of arc current.

Using Model 3, two additional tests were conducted. The first was a study of total ion current and  $D^+$  percentage vs. magnetic field strength. At 8.0 Pa source pressure, variation of the magnet current from 1.5 A to 2.5 A (magnetic flux near intermediate electrode increased from 0.12 T to 0.17 T) resulted in a total ion current increase from 176 mA to 210 mA, respectively. However, the percent  $D^+$  remained constant.

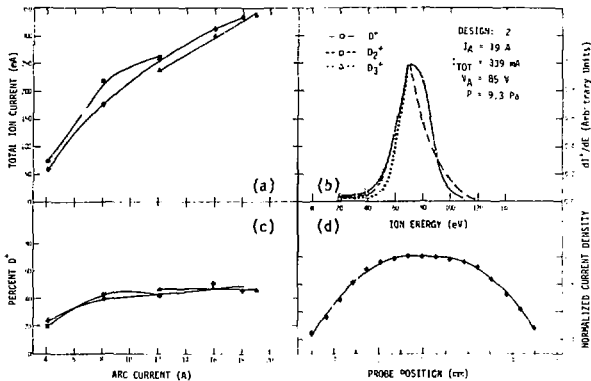


Figure 3. Experimental Data Obtained on Duopigatron - Model 2.

- (a) Total current vs. arc current for three source pressures; ■ 6.7 Pa, ◆ 8.0 Pa, ▲ 9.3 Pa.
- (b) Ion energy distributions for 19 A arc current and 9.3 Pa source pressure. Energy measured relative to cathode potential.
- (c) Percent  $D^+$  vs. arc current for three source pressures; ■ 6.7 Pa, ◆ 8.0 Pa, ▲ 9.3 Pa.
- (d) Ion current density distribution in  $Z = 0$  plane of plasma expansion cup for 15 A arc current and source pressure of 8.0 Pa.

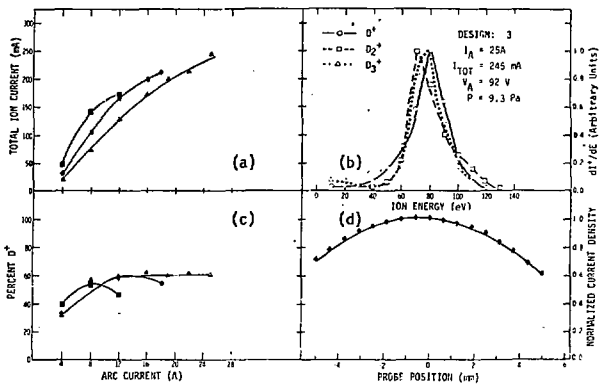


Figure 4. Experimental data obtained for duopigatron - Model 3; notation as in Fig. 3, refer to figure legend for (b).

The second test was an attempt to reduce secondary cathode sputtering by operating the secondary cathode at plasma floating potential. The result was a markedly smaller  $D^+$  fraction (about 30%) which precluded the floating configuration from further consideration.

#### D. Model 4.

The fourth source design had its intorelectrode spacings reversed from those of Model 3; i.e.,  $S_1$  was reduced to 12.7 mm and  $S_2$  was increased to 30.5 mm. The purpose of this test was to determine if moving the anode closer to the cathode while keeping the overall arc length constant had any appreciable effect on the ion production characteristics. As shown in Table 1 and Fig. 5, the effects were small. There were small decreases in total ion current, small increases in atomic ion percentage, and slightly more peaked ion current density distributions. One significant result of the two tests with the steel secondary cathode (Models 3 and 4) was that the steel was severely eroded causing insulators in the ion source to be coated with metal. Such erosion would probably introduce metal ion contaminants to the ion beam which would cause intolerable sputtering of the target in a neutron generator. For this reason, the steel secondary cathode was eliminated from further consideration. However, it was obvious from the first four models tested that the steel in the secondary cathode region improved the ion current density profile.

#### E. Model 5.

This model incorporated a copper secondary cathode with a molybdenum insert. An all steel plasma expansion cup (12.7 mm id, 15.2 mm deep) without a DN insert was used in an attempt to obtain a flatter ion current density profile than observed with Models 1 and 2. Electrode spacings were the same as for Models 2 and 3. A summary of the data from this source is shown in Fig. 6. A total ion current of 200  $\mu$ A was obtained with an arc current of 26 A at a source pressure of 10.1 Pa. Ion energy distributions were similar to those presented earlier. Atomic ion percentages at arc currents greater than 12 A were 60 to 65%. The ion current density profile at  $Z = 0$  was peaked at the center of the cup and fell off to 80% of the peak value at the cup walls. The data at 20 A arc current and 9.3 Pa source pressure are summarized in Table I.

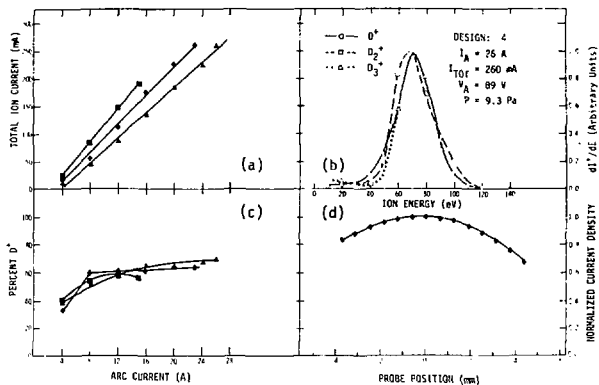


Figure 5. Experimental data Obtained for Duopigatron - Model 4; notation as in Fig. 3, refer to figure legend for (b).

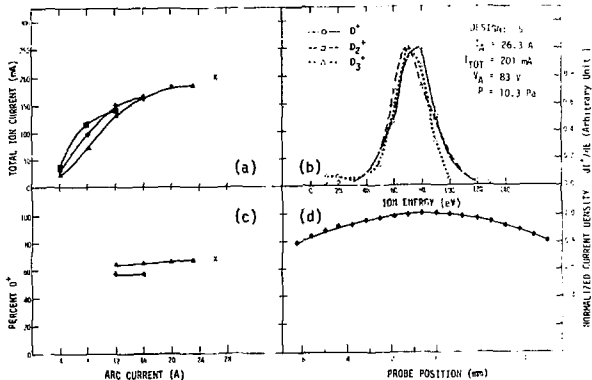


Figure 6. Experimental Data Obtained on Duopigatron - Model 5.

- Total ion current vs. arc current for four source pressures;  $\blacksquare$  6.7 Pa,  $\blacklozenge$  8.0 Pa,  $\blacktriangle$  9.3 Pa,  $\times$  10.1 Pa.
- Ion energy distributions relative to cathode potential.
- Percent  $D^+$  vs. arc current for three source pressures;  $\blacklozenge$  8.0 Pa;  $\blacktriangle$  9.3 Pa;  $\times$  10.1 Pa.
- Ion current density distribution in  $z = 0$  plane of plasma expansion cup for 20 A arc current and source pressure of 9.3 Pa.

F. Models 6 and 7.

The next two models were tested to determine how the length of the arc discharge affected the ion production characteristics. For these tests, the 12.7 mm long insulator was exchanged for one 38.1 mm long and the source was examined with the long insulator in first the  $S_2$  position then the  $S_1$  position, for Models 6 and 7, respectively. Results for 20 A arc current and 9.3 Pa source pressure are shown in Table 1 and Figs. 7 and 8. The total ion current was reduced from the previous test to 120 to 130 mA and the atomic ion percentage increased to about 70%. The ion current density profiles were about the same as for Model 5. Over the arc current range of 12 to 24 A, the atomic percentage was 60 to 70% and the ion current varied from 60 to 160 mA for Model 6 and 50 to 180 mA for Model 7 at a source pressure of 9.3 Pa.

G. Models 8, 9, and 10.

The last three models were tested to determine how the depth of the plasma expansion cup affected the ion production characteristics. For these tests,  $S_1$  was 12.7 mm,  $S_2$  was 30.5 mm, and the steel cup was 15.2, 7.6, and 11.5 mm deep for Models 8, 9, and 10, respectively. For 20 A arc current and a source pressure of 9.3 Pa, the shallow cup gave the most beam current and the most peaked ion current density distributions. The product of the total ion current in amperes,  $I^+$ , and the ratio R, defined in Table 1, is given as

$$I^+R = 0.11$$

for the above operating conditions. For these models

$$R = 0.045 d$$

where  $d$  is the depth of the plasma expansion cup in mm. Under the operating conditions shown in Table 1, the atomic percentage was independent of cup depth; however, the atomic ion percentage was about 50% for the 7.6 mm deep cup at arc currents of 12 A and 16 A while remaining near 60% for the two deeper cups. Results for the different experiments are shown in Figures 9, 10, and 11.

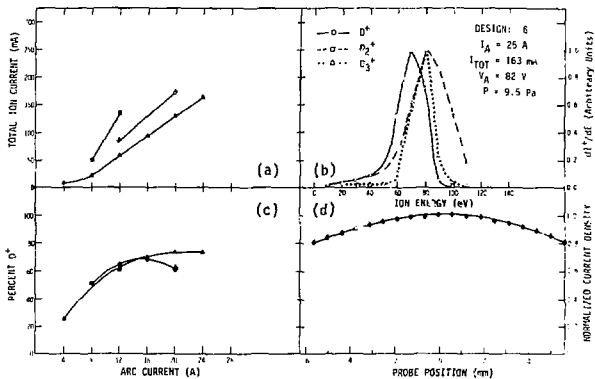


Figure 7. Experimental Data Obtained for Duopigatron - Model 6; notation as in Fig. 3, refer to figure legend for (b).

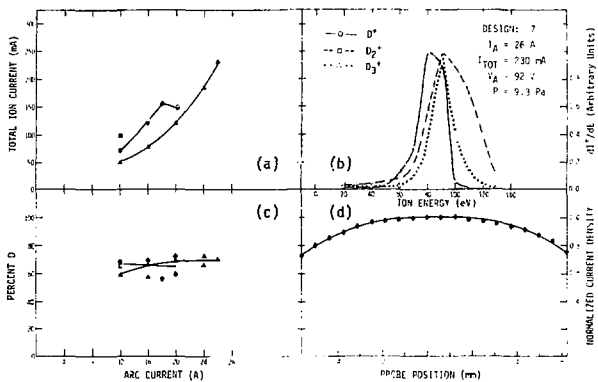


Figure 8. Experimental Data Obtained for Duopigatron - Model 7; notation as in Fig. 3, refer to figure legend for (b).

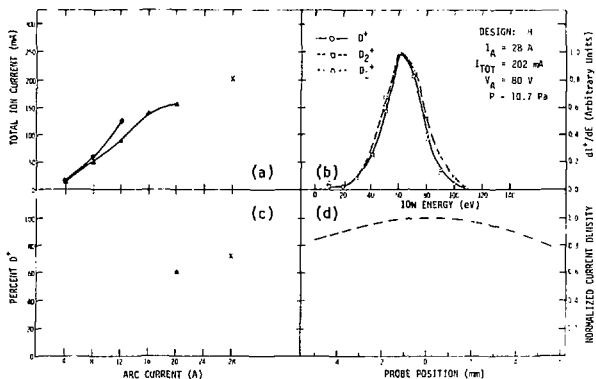


Figure 9. Experimental Data Obtained for Duopigatron - Model B.

- Total current vs. arc current for three source pressures;  $\blacklozenge$  8 Pa,  $\blacktriangle$  9.3 Pa,  $\times$  10.7 Pa.
- Ion energy distributions for 28 A air current and 10.7 Pa. Energy measured relative to cathode potential.
- Percent  $D^+$  vs. arc current for two source pressures;  $\blacktriangle$  9.3 Pa,  $\times$  10.7 Pa.
- Estimated ion current distribution in  $Z = 0$  plane of plasma expansion cup.

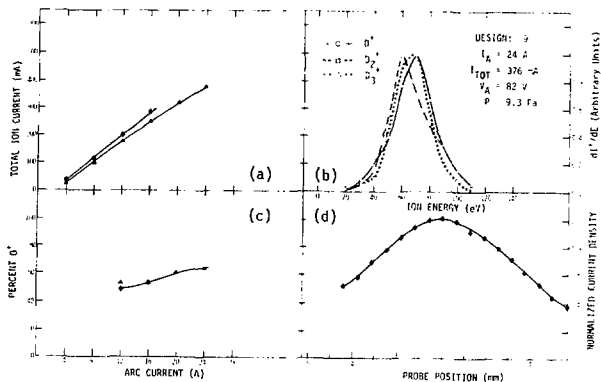


Figure 10. Experimental Data Obtained for Duopigatron - Model 9.

- Total current vs. arc current for two source pressures;  $\blacklozenge$  8 Pa,  $\blacktriangle$  9.3 Pa.
- Ion energy distributions for 24 A arc current and 9.3 Pa. Energy measured relative to cathode potential.
- Percent  $D^+$  vs. arc current for two source pressures;  $\blacklozenge$  8 Pa,  $\blacktriangle$  9.3 Pa.
- Ion current density distribution in  $Z = 0$  plane of plasma expansion cup for 16 A arc current and source pressure of 8.0 Pa.

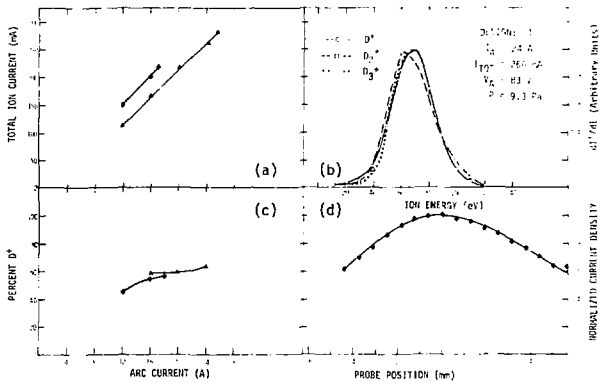


Figure 11. Experimental Data Obtained for Duopigatron - Model 10; notation as in Fig. 10, refer to figure legend for (b).

#### IV. DISCUSSIONS AND CONCLUSIONS

Of the configurations tested, the copper secondary cathode with the molybdenum insert and the all steel plasma expansion cup gave the best results. An ion current density profile that was peaked at the center of the cup and fell to 80% of the peak value at the plasma expansion cup walls was obtained with a steel cup 15.2 mm deep by 12.7 mm inside diameter. Total ion currents approaching 200 mA containing 60 to 70%  $D^+$  were produced with this configuration (see data of Model 5 in Fig. 6). Larger beam currents could be produced by decreasing the cup depth; however, this produced a more sharply peaked ion current density distribution. The ratio of the current density at the edge of the plasma expansion cup to that at the cup center was found to be approximately proportional to the cup depth over the range of 7.6 to 15.2 mm. As the cup depth was varied over this range, the product of the beam current and the above ratio was found to be approximately constant for constant ion source pressure and arc current. Interelectrode spacings were found to have an effect on the beam current and mass distribution. The larger spacings tested produced the higher atomic ion fraction but lower total beam currents.

The ion current density distribution was much more sharply peaked, and the total current was about twice as large for the steel plasma expansion cup with the boron nitride insert than for the all steel expansion cup. These data are consistent with a model previously proposed for the duoplasmatron<sup>1</sup> where the plasma tends to expand along the magnetic field lines. In the case of the cup with the boron nitride insert, the magnetic field lines near the axis of the ion source were only weakly affected by the cup and the plasma density remained sharply peaked on the axis and fewer plasma losses occurred at the cup walls. For the all steel cup, the magnetic field lines were pulled into the cup walls which caused the plasma density profile to flatten and increased plasma losses at the wall.

The all steel secondary cathode with the steel and boron nitride expansion cup produced a plasma with characteristics somewhere between

those of the previous two configurations. The current density profile was flatter and the ion current was lower than with the Cu/Mo secondary cathode and the steel/BN expansion cup. Compared to the Cu/Mo secondary cathode and the all steel expansion cup, this configuration produced a more sharply peaked ion current density distribution and a slightly larger beam current.

#### LIST OF REFERENCES

1. F. M. Bacon, "Gas Discharge Ion Source. I. Duoplasmatron," Rev. Sci. Instr. 49, 427 (1978).
2. R. A. Demirkhanov, Yu. V. Kursanov, and V. M. Blagoveschenskii, Instr. and Exp. Tech. 1, 25 (1964).
3. O. B. Morgan, G. G. Kelley, and R. C. Davis, Rev. Sci. Instr. 38, 467 (1967).
4. F. M. Bacon, R. W. Bickes, Jr., and J. B. O'Hagan, "Gas Discharge Ion Source. II Duopigatron," Rev. Sci. Instr. 49, 435 (1978).
5. J. E. Boers and R. J. Walko, Bull. Am. Phys. Soc. 21, 1030 (1976).